Microwave Amplifiers Employing Integrated Tunnel-Diode Devices

HERMAN C. OKEAN, SENIOR MEMBER, IEEE

Abstract—**A series of shunt-tuned integrated microwave tunnel-diode devices utilizing unencapsulated beam lead tunnel diodes and including tuning and stabilizing circuitry have been fabricated using tantalum thin-film technology for use as the active element in microwave reflection amplifiers. The theoretical properties of such devices have been explored, and data relating to their design and measured performance are presented in detail. Finally, the successful use of these devices as the active elements in a series of absolutely stable circulator-coupled reflection amplifiers at 4 and 6 GHz has been demonstrated.**

Introduction

THE RELATIVE simplicity and moderately low noise capability of microwave tunnel-diode amplifiers leads to their frequent use as low-level preamplifiers in microwave receiving systems.[1]–[7] These amplifiers usually employ, in close association with the tunnel diode, one or more reactive tuning elements and a band-rejection type stabilizing network.[6]–[8] To provide effective tuning and stabilization, this circuitry must be physically and electrically as close to the tunnel-diode junction as possible and should be electrically "lumped" over the entire active frequency range of the tunnel diode. These objectives are often difficult to accomplish using conventional microwave circuit realizations and encapsulated tunnel diodes.

Therefore, this paper will describe the integration of an unencapsulated tunnel diode, a reactive tuning element, and a stabilizing network, using thin-film technology, into a single stabilized and tuned active bandwidth-limited negative resistance device[9] of size comparable to most existing encapsulated tunnel diodes, and the use of such devices in microwave reflection amplifiers. This approach satisfies these objectives and provides the added advantages of small size and weight and potential mass reproducibility.

The paper begins with a summary of the theoretical properties of a particular tuned and stabilized integrated tunnel-diode device (ITDD), as used in a circulator-coupled reflection amplifier. The design and realization of a family of such devices is then described in detail. Finally, results are presented on the utilization of these devices in a series of 4 GHz tunnel-diode amplifiers and in a 6 GHz tunnel-diode amplifier.

Manuscript received March 2, 1967; revised June 28, 1967.

The author was formerly with Bell Telephone Labs., Inc., Murray Hill, N. J. He is currently with the Airborne Instruments Lab., A Division of Cutler-Hammer, Inc., Melville, L. I., N. Y. 11749

Theoretical Properties of Amplifiers Using ITDD

ITDD Equivalent Circuits

Electrically, the ITDD consists of a tunnel diode in combination with its reactive tuning element and a stabilizing network. Whereas four possible ITDD configurations are theoretically possible[1] (shunt or series tuning and shunt or series stabilizing), the configuration to be considered here[1] utilizes a tuning element and stabilizing network which are both connected in shunt with the tunnel diode.

The exact small signal equivalent circuit of a representative ITDD is presented in Fig. 1(a) along with the basic equations relating the element values. In addition, the simplified equivalent circuit of Fig. 1(b) is valid in the vicinity of device center frequency ω_0,[8] provided the tunnel-diode series inductance L is less than some $L_{max} \approx 2RCR_s$ and if $\omega_0 < 0.3\ \omega_R$, conditions which usually can be satisfied using unencapsulated, high resistive cutoff frequency (ω_R) tunnel diodes.

In the exact circuit, shunt-tuning inductor L_t resonates the net diode capacity at ω_0 and blocking capcitor C_b, essentially zero reactance at ω_0, prevents the short circuiting of the externally applied dc diode bias voltage.

Performance Capabilities of Reflection Amplifiers Utilizing ITDD

The gain-bandwidth, stability, and noise-figure characteristics of circulator-coupled negative-resistance reflection amplifiers have been treated extensively in the literature.[6],[8],[11] We consider here such an amplifier utilizing an ITDD as the negative-resistance element connected to the amplifier arm of the circulator through a lossless cou-

[1] Four possible ITDD circuit configurations exist, each having connected to a tunnel diode: a) a series or parallel inductor to resonate capacitive tunnel-diode reactance at the device center frequency ω_0, and b) a single stage resistively terminated, series or parallel band rejection resonator, tuned to ω_0, having an input impedance or admittance, respectively, which appears reactive for $\omega \sim \omega_0$ and resistive for $\omega \gg \omega_0$ and $\ll \omega_0$. The four configurations are: parallel tuned parallel stabilized (PTPS), parallel tuned series stabilized (PTSS), series tuned parallel stabilized (STPS), and series tuned series stabilized (STSS). Of these, the ST devices are inherently harder to stabilize and are more sensitive to variations in diode parameters, but can accommodate larger values of diode series inductance. The PTSS and STPS devices are generally more difficult to incorporate into reflection amplifiers than the STSS and PTPS devices.[8] Over all, assuming the availability of low inductance tunnel diodes, the PTPS configuration seems to be optimum and will be considered exclusively here.

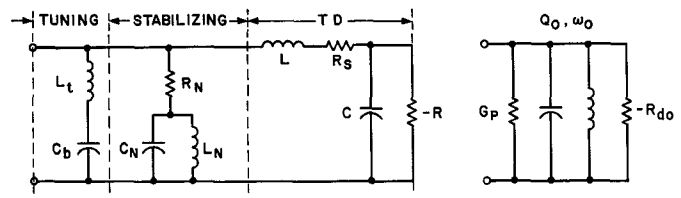

Assume

$k=(L/RCR_s)\lesssim 2$

$\omega_0=\dfrac{1}{\sqrt{L_NC_N}}\gg\dfrac{1}{\sqrt{L_tC_b}}$

$\alpha_0=\left(\omega_0RC\Big/\sqrt{\dfrac{R}{R_s}-1}\right)\lesssim 0.3.$

Then, in terms of the required Q_N and R_N

$$C_N=Q_N/\omega_0R_{d0}$$

$$L_N=\frac{R_{d0}}{\omega_0Q_N}.$$

In addition

$$L_t=1/\omega_0^2C_{d0}$$

R_{d0}, C_{d0} = passband TD parameters

(a) Exact equivalent circuit.

$R_{d0}\approx(R-R_s)(1-k\alpha_0^2)$

$C_{d0}\approx CR/R_{d0}$

$Q_0=Q_N+\omega_0R_{d0}C_{d0}$

G_p = loss conductance at ω_0 due to R_N, L_N, C_N, L_t, and C_b ($G_NR_{d0}\ll 1$).

(b) Approximate passband equivalent circuit.

Fig. 1. ITDD small signal equivalent circuits.

TABLE I

ITDD Performance in Circulator-Coupled Reflection Amplifier

Half-power nth order maximally flat amplification bandwidth

$$\beta=\frac{\omega^+-\omega^-}{\omega_0}=\frac{2(\Gamma_0^2-2)^{-1/2n}\sin\dfrac{\pi}{2n}}{Q_0(1-\Gamma_0^{-1/n})}$$

Midband noise figure

$$F\approx L_c\left[1+\frac{\Gamma_0^2-1}{\Gamma_0^2(1-G_pR_{d0})}\left(\frac{20IR+\alpha^2+\delta(1-\alpha^2)}{(1-\delta)(1-\alpha^2)}+G_pR_{d0}\right)\right]$$

Maximum "active" bandwidth of ITDD

$$\beta_A=\frac{\omega_A^+-\omega_A^-}{\omega_0}=\left[\omega_0R_NC_N\sqrt{\frac{R_{d0(\min)}}{R_N}}-1\right]^{-1}$$

where

I = dc diode bias current

$\delta=R_s/R$; $\alpha^2=\omega_0^2R^2C^2\delta/(1-\delta)$

Γ_0^2 = midband power gain

L_c = circulator forward loss per pass

β assumes that diode is the bandwidth limiting element[8]

and where

circuit parameters are as defined in Fig. 1.

pling network. The ITDD circuit models of Fig. 1(a) and (b) are then applied to existing formulations[8]–[11] to yield expressions for amplification bandwidth, active bandwidth, and noise figure of an ITDD reflection amplifier as summarized in Table I. The primary points of significance in Table I are as follows.

1) The degradation in amplification bandwidth due to the presence of Q_N in Q_0 (Fig. 1) is often not important in practical cases in which the circulator is the bandwidth limiting element.[8]
2) The active bandwidth of the ITDD (over which it presents a negative input conductance) is equated to the stability bandwidth of the given amplifier configuration[8] in order to determine the required Q_N for a convenient choice of $R_N<R_{d0}$ (min).
3) Loss conductance G_P consists of components due to conductor and dielectric losses in the nominally lossless elements L_N, C_N, C_b, and L_t as well as the band edge contribution due to R_N. Since the circuit losses generally increase with increasing Q_N, a circulator with poor out-of-band characteristics, thus requiring a high Q_N, can indirectly degrade the amplifier noise performance due to the high resulting G_P.

Design and Realization of ITDD Series for Amplifier Use at 4 and 6 GHz

Basic Physical Configuration

A successful physical realization of the ITDD discussed in the preceding section for use at 4 and 6 GHz is shown in Fig. 2. It is basically a hybrid integrated circuit utilizing tantalum thin-film techniques on a ceramic substrate. It consists of a germanium beam lead tunnel diode bonded across the parallel combination of a thin-film stabilizing network and a thin-film tuning branch. Each diode bond is formed by a split tip or ultrasonic welded joint or a drop of conductive epoxy. The entire thin-film circuit is deposited on a 0.162 inch long, 0.188 inch wide, and 0.031 inch thick sapphire substrate.

The resulting hybrid integrated circuit utilizes well-established tantalum thin-film techniques.[12],[13] In particular, the thin-film stabilizing network consists of a 5 mil square tantalum thin-film resistor R_N in series with the parallel L_N–C_N circuit, resonant at ω_0. The L_N–C_N circuit is composed of an 8 by 5 mil overlap "parallel plate" capacitor C_N utilizing a silicon monoxide dielectric, shunted by a coupled stripline inductive loop. The tuning inductor L_t is an inductive loop connected to ground through a 35 by 12 mil overlap blocking capacitor C_b of configuration similar to C_N. The thin-film lumped circuitry is situated in a 20 mil gap between a thin-film 50 ohm input conductor and a thin-film ground contact area which form the contacts to the external circuitry and to ground, respectively.

The well-documented tantalum thin-film fabrication process[12],[13] such as used on the ITDD may be summarized briefly as follows, with reference to Fig. 3.

1) Define the conductor pattern, resistor area, and capacitor area by application of a photoresist process and selective etching to a composite tantalum nitride (35 ohms per square) chrome–gold 3000 Å film deposited on the top surface of the sapphire substrate [Fig. 3(a)].
2) Define resistor R_N by further etching and photoresist processing of the desired resistor area [Fig. 3(b)].
3) Electroplate conductor areas with copper to a thickness of about 0.2 mil ($\approx$5 skin depths at 4 GHz, $\approx$6 at 6 GHz), following it up with a 0.01 mil gold flash [Fig. 3(c)].

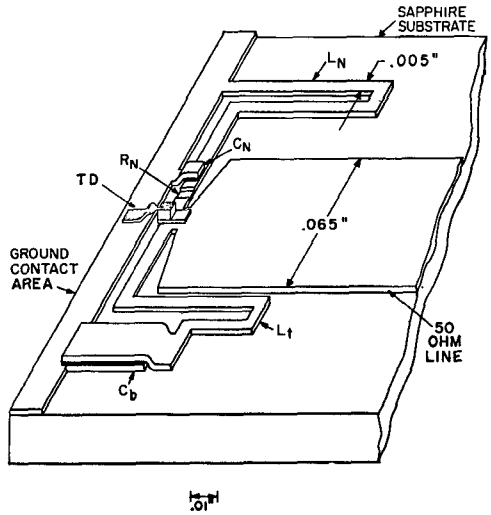

Fig. 2. Physical realization of thin-film ITDD on sapphire substrate.

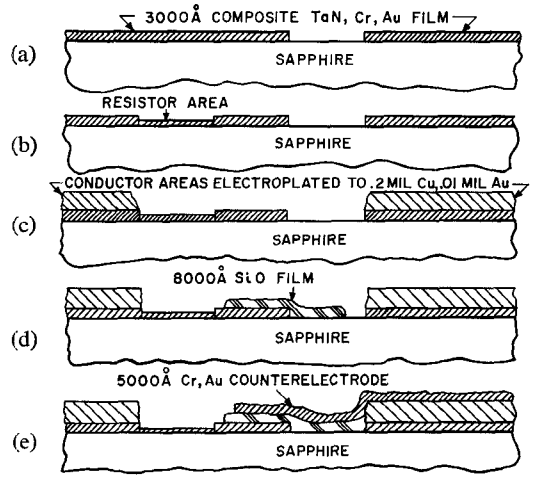

Fig. 3. Fabrication process for tantalum thin-film circuitry on ITDD.

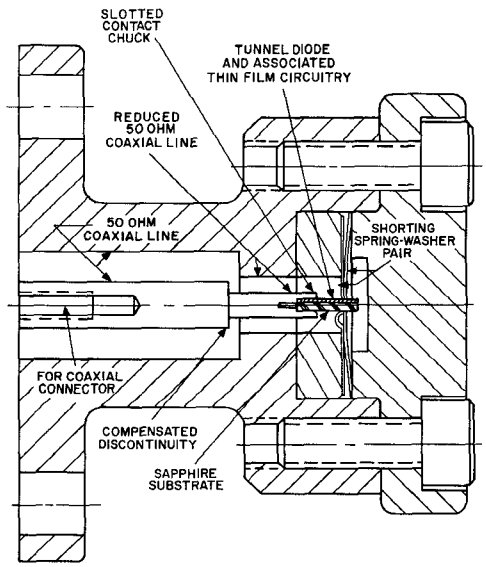

Fig. 4. One-port coaxial mounting fixture for ITDD.

4) Evaporate an 8000 Å SiO dielectric on the capacitor base electrode area [Fig. 3(d)].
5) Evaporate a chrome–gold 5000 Å counterelectrode to form the top electrode of the capacitor [Fig. 3(e)].

Mounting Fixtures for ITDD

The ITDD may be mounted in a conventional transmission-line structure for characterization or use in an amplifier or it may be formed on a larger substrate containing the remaining thin-film components (or bulk components such as ferrites) required to realize a completely integrated amplifier. A 50 ohm coaxial "one-port" mounting fixture used both for characterizing completed integrated devices and related thin-film circuits and for incorporating integrated devices in coaxial amplifier structures is shown in Fig. 4.

The mount utilizes a slotted contact chuck in the 65 mil diameter 50 ohm cylindrical center conductor to contact the 50 ohm thin-film line on the substrate, and a combination of leaf and belleville springs to apply a solid dc and RF ground at the leading edge of the ground contact area. The substrate rests in slots in the cylindrical outer conductor and is held in place by the contact chuck and the springs. The compensated step in the dimensions of the inner and outer conductor of the coaxial line is of standard design.[14]

The mismatch in the mount due to this step and to the transition from the 50 ohm coaxial line to the 50 ohm thin-film line at the contact chuck is estimated from reflection measurements as exhibiting a VSWR <1.09 with respect to a 50 ohm termination over the 3 to 5 GHz range.

Realization of Thin-Film Circuit Elements

The realization of the ITDD configuration described above was preceded and accompanied by a design study on the various thin-film circuit elements comprising the ITDD. This included an evaluation of the characteristic impedance and effective dielectric constant of thin-film transmission line in the cylindrical mount geometry, and the derivation of the microwave equivalent circuits and of design information for lumped thin-film resistors, capacitors, and inductors. The results of this study are as follows.

Thin-Film Transmission Line: The TEM transmission line used on the ITDD consists of a thin-film strip center conductor on the given sapphire substrate (Fig. 2) coaxial with a cylindrical outer conductor formed by the given mount geometry as shown in Fig. 4. The characteristic impedance Z_0 and the effective dielectric constant $\tilde{\epsilon}$ of this somewhat unusual transmission-line configuration have been determined theoretically and verified experimentally as functions of center conductor width w, cylindrical outer conductor diameter, and substrate thickness and dielectric constant.[15] As a result of this characterization, the nominal 50 ohm center conductor ($w=0.065$ inch) yields an input VSWR of less than 1.15 over 2.0 to 7.5 GHz and an $\tilde{\epsilon}\approx 3.5$ when mounted in a 50 ohm terminated fixture[16] of outer conductor geometry (0.149 inch diameter) identical to that of Fig. 4.

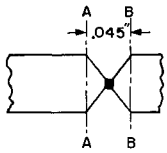

A to A = input impedance plane
B to B = plane of ground contact

(a) Thin-film resistor configuration.

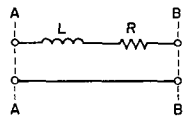

Typical measured values

$R \approx 30.5$ ohms (2 to 6 GHz)

$L \approx 0.45$ nH

$R_{dc} = 29.8$ ohms

(b) Thin-film resistor equivalent circuit.

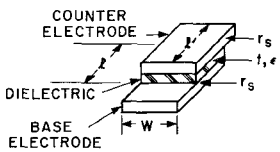

$$C(\text{pF}) \approx 0.225\epsilon \frac{l(\text{in})W(\text{in})}{t(\text{in})}$$

$$R_s \approx \frac{r_s}{W}\left[\frac{2}{3}l + (l' - l)\right]$$

Typically,

$t \approx 0.00003$ inch

$\epsilon \approx 6$

$r_s \approx 1.0$ ohms/square

(c) Thin-film capacitor configuration.

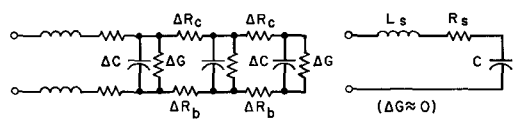

(d) Exact equivalent circuit. (e) Simplified equivalent circuit.

CAPACITOR	C_N	C_b
l – in	.005	.035
W – in	.008	.012
CALCULATED C – pF	1.8	19.0
L F MEASURED C – pF	1.96	—
R F MEASURED C – pF	1.98	19.8 (AV)
l' – in	.009"	.038"
CALCULATED R_s – OHMS	0.28	0.60
MEASURED R_s – OHMS	0.50	1.2 (AV)

(f) Tabulation of capacitor parameters.

Fig 5. Thin-film resistive and capacitive element configurations and equivalent circuits.

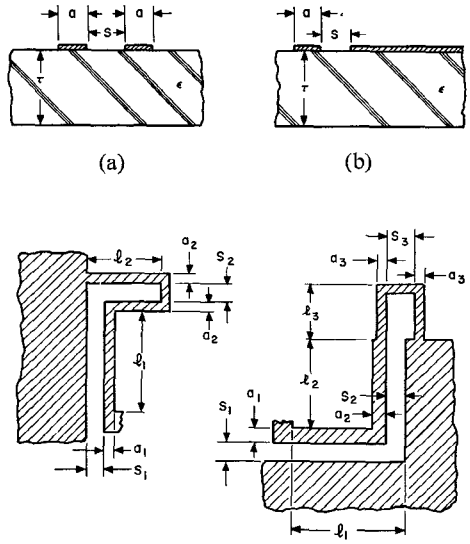

Typically,

$S_1 = 0.004$ inch

$a_1 = a_2 = S_2 = 0.005$ inch

$l_1 = 0.0295$ inch

$l_2 = 0.0215$ inch

(c)

Typically,

$a_1 = a_2 = S_3 = 0.005$ inch

$a_3 = 0.003$ inch

$S_2 = S_1 = 0.004$ inch

$l_1 = 0.050$ inch

$l_2 = 0.030$ inch

$l_3 = 0.009$ to 0.034 inch

(d)

Fig. 6. Thin-film inductor configurations. (a) and (b) Coupled-strip inductor cross sections. (c) and (d) Thin-film inductor realizations.

Thin-Film Resistors: The basic thin-film resistor consists of a tantalum film rectangle of length L, width W, and surface resistivity K ohms per square, yielding a resistance of $K(L/W)$ ohms, For the given realization, $L = W = 0.005$ inch and the resulting resistance range is 20 to 50 ohms. The microwave impedance of such a resistor formed in series in a 50 ohm thin-film transmission line [Fig. 5(a)], mounted as in Fig. 4, is essentially that of the dc resistance of the resistive film in series with the inductance of the shorted length of 50 ohm transmission line between the resistor and ground, as shown for a typical resistor in Fig. 5(b). Therefore, the RF impedance of the film resistor itself is basically the lumped dc resistance.

Thin-Film Capacitors: To obtain sufficient capacitance per unit area to meet the ITDD circuit requirements, the parallel plate overlap capacitor configuration of Fig. 5(c), including nominal dimensions and capacitance values, is used for capacitors C_b and C_N in the ITDD realization. The exact equivalent circuit of such a structure including dielectric and conductor losses in the base and counter electrodes is that of a distributed RC line as shown in Fig. 5(d). If the only significant losses are conductor losses in the electrodes, as is the case for the capacitors used in the ITDD realization, the exact circuit simplifies[16] to that of Fig. 5(e). The validity of the lumped circuit of Fig. 5(e) at microwave frequencies is borne out by the measured impedance loci of typical C_b and C_N realizations which yield equivalent circuit values in good agreement with the theory, as shown in Fig. 5(f).

Thin-Film Inductors: A thin-film inductor realization which is relatively independent of the given outer conductor geometry is that of a short-circuited coupled-strip transmission line. Two possible coupled stripline cross sections are shown in Fig. 6(a) and (b) and two inductor realizations utilizing them are presented in Fig. 6(c) and (d). The characteristic impedance of the coupled striplines of Fig. 6(a) and (b) is presented in the Appendix, based on previous work,[17],[18] and is applied therein to the calculations of the

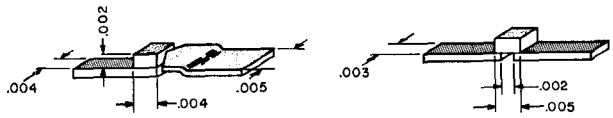

(a) Simulated beam lead diode. (b) Planar diode.

Fig. 7. Unencapsulated beam lead tunnel diodes.

TABLE II

MEASURED SMALL SIGNAL PARAMETER VALUES OF UNENCAPSULATED TUNNEL DIODES

Parameter	Diode		Measurement
	Pulse Bonded*	Planar*	
R_{min} ohms	60–85	70–126	A, B
$R(V_{op})$ ohms**	70–105	100–136	A
R_s ohms	2.7–4.0	—	C, E
$C(V_v)$ pF	0.50–1.05	0.59–1.02	D, E
$C(V_{op})$ pF**	0.40–0.85	0.41–0.79	D
L nH	0.15–0.20	—	E
V_{op} mV**	102–126	136–150	A
$IR(V_{op})$ mV**	50–77	64–78	A

A = static I–V characteristic $R = \left|dI/dV\right|_{V_0}^{-1} + R_s$
B = 1 kHz measurement of dV/dI
C = audio frequency measurement of dV/dI under reverse bias
D = 100 MHz capacitance bridge measurement for $C(V_v)$

$$C(V_{op}) = C(V_v)\sqrt{\frac{620 - V_v(\text{mV})}{620 - V_{op}(\text{mV})}}$$

E = microwave (2.0 to 7.5 GHz) slotted line immittance measurement with input signal applied to slotted line probe
* 85 pulse bonded diodes, 4 planar diodes
** V_{op} for compromise between lowest IR and best large signal operation.[6]

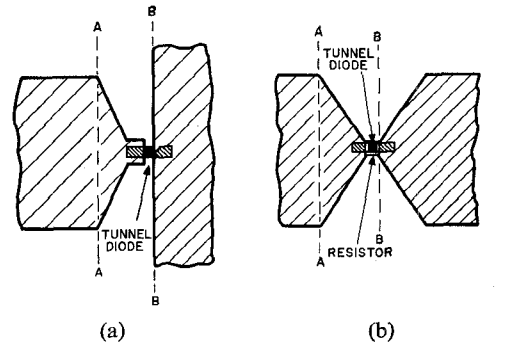

(a) (b)

A to A: reference plane for input immittance measurements
B to B: ground contact reference plane

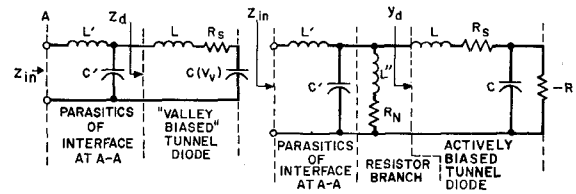

$$z_d = \left[\frac{1}{Z_{in} - j\omega L'/R_0} - j\omega C' R_0\right]^{-1}$$

$L' \approx 0.27$ nH

$C' \approx 0.15$ pF

$R_0 = 50$ ohms

V_V = valley bias voltage

(c)

$$y_d = \frac{1}{Z_{in} - j\omega L'/R_0}$$

$$\frac{R_0}{R_N + j\omega L''} - j\omega C' R_0$$

$L' = 0.20$ nH

$C' = 0.15$ pF

$L'' = = 0.25$ nH

$R_0 = 50$ ohms

(d)

Fig. 8 Characterization of unencapsulated tunnel diodes on thin-film circuits. (a) and (b) Thin-film circuit configurations for tunnel-diode characterization. (c) and (d) Equivalent circuits for determination of tunnel-diode parameters.

inductances of Fig. 6(c) and (d). Microwave impedance measurements on such inductors indicate a loss resistance in series with an inductive reactance as predicted in the theory in the Appendix. A comparison of theoretical and measured values of inductance and loss resistance as functions of dimension are presented in Table VI in the Appendix. The consistently lower values of measured inductance in comparison with theory may be attributed to the lowering of the characteristic impedance of a given coupled stripline due to coupling to the distant but not infinitely removed cylindrical outer conductor.

Unencapsulated Tunnel Diodes for ITDD

The unencapsulated tunnel diode used in the nominal ITDD realization is a simulated beam lead germanium diode [Fig. 7(a)] developed at the Bell Telephone Labs. It consists of a 2 by 4 by 4 mil germanium block, to an edge of which is pulse bonded a pointed lead-antimony ribbon, thereby forming the diode junction. The junction is strengthened mechanically by the addition of a drop of epoxy. The other contact consists of a 4 mil wide gold plated kovar ribbon which is bonded to the bottom of the germanium wafer.

This diode is the forerunner of a planar beam lead germanium tunnel diode [Fig. 7(b)] recently developed at the Bell Telephone Labs.[19] for possible use in the ITDD. The planar diode consists of a 5 by 5 by 2 mil germanium block, to the bottom face of which are alloyed a small (~0.1 mil²) and a large (~6 mil²) tin-arsenic film dot. The small dot forms the tunnel-diode junction and the large dot an essentially ohmic contact to the germanium. Beam leads attached to each of the films comprise the diode contacts.

Typical small signal parameter ranges[2] for both types of tunnel diodes, based on low frequency and microwave measurements, are listed in Table II. The diode is characterized at RF by measuring the input immittance of a valley biased ($R = \infty$) or actively biased diode, bonded across appropriate thin-film circuits [Fig. 8(a) and (b)], each on a sapphire substrate, mounted as in Fig. 4. The valley biased diode [Fig. 8(a)] is bonded across a 4 mil gap between a 50 ohm thin-film transmission line and a ground contact area identical to those encountered in the ITDD (Fig. 2). The actively

[2] Any stray capacitance between the beam leads is sufficiently small and sufficiently close (electrically) to the diode junction to be considered to a good approximation and to be part of the junction capacitance.

biased diode [Fig. 8(b)] is bonded across a thin-film resistor in series with a 50 ohm line such as described in Fig. 5, the resistor serving to stabilize the actively biased diode.

In each configuration, it was found that the discontinuity between the 50 ohm thin-film input line and the lumped circuitry external to the tunnel diode was representable by a series inductance L' and shunt capacitance C' at the desired reference plane, as shown in Fig. 8(c) and (d). Note that L' and C' are not to be considered parasitics of the tunnel diode since, in the ITDD, they are external to both the stabilizing and tuning branches. The extraction of the tunnel-diode immittance data from the measured immittance data is accomplished using Fig. 8(c) and (d), and the relevant diode parameters are obtained using appropriate curve fitting. The most significant conclusions drawn from the diode characterizations (Table II) are as follows.

1) The total series inductance of the diode, excluding the external discontinuity inductance L' [Fig. 8(c)], measures 0.15 to 0.20 nH in the given ITDD geometry. This compares as expected with the value of 0.1 nH obtained with the diode in Fig. 8(a) replaced by a 5 mil wide lead strap.
2) The total RF series resistance of the diode, including contact resistance, is approximately the dc value plus 1.0 ohms.
3) The planar diode of a given negative resistance level has a higher series resistance, shot-noise constant, and peak and valley voltage than its simulated beam lead counterpart.

ITDD Design and Characterization

The design of the ITDD configuration of Fig. 2 is based on the design information obtained for individual thin-film circuit elements, the measured RF parameters of representative tunnel diodes, and the active bandwidth requirements[8] established for particular amplifier designs using specified circulators. Using measured circulator and diode data, the nominal thin-film circuit element design values are determined in the next section and presented in Table III for particular 4 and 6 GHz ITDD designs. Note that the 4 GHz design makes provision for several different values of tuning inductance L_t(*E-H*) in order to accommodate a wide range (0.5 to 1.0 pF) of diode terminal capacitance. The required dimensions for the realizations of the various thin-film circuit elements having the specified design values listed in Table III are determined using the theoretical and measured design information contained in the preceding section. Typical values are shown in Figs. 5 and 6. The calculated total ITDD shunt-loss conductances based on these dimensions are also presented in Table III.

The individual thin-film circuit element values obtained in practice in the realization of the ITDD configuration of Fig. 2 may be extracted from measurements of the input immittance of the ITDD, mounted as in Fig. 4, prior to bonding the tunnel diode to the ITDD, using straightforward circuit analysis. The statistical breakdown on the measured element values, including total loss conductance of 290 4-GHz ITDD circuits and two 6-GHz circuits provided in Table III, indicates a generally successful realization of the ITDD design.

TABLE III
ITDD THIN-FILM CIRCUIT ELEMENT VALUES

Element	Model	Nominal Design Value	Measured Values		
			Range	Average	Sample Size
R_N ohms	All	30.0	20–42	31.0	290
C_b pF	All	20.0	17.1–22.6	18.5	7
C_N pF	C	1.0	0.98–1.04	1.01	2
	E–H	2.5	1.7–3.5	2.54	290
L_N nH	C	0.7	0.62–0.74	0.68	2
	E–H	0.65	0.43–0.85	0.62	290
L_t nH	C, E	1.40	1.1–1.6	1.36	77
	F	1.70	1.2–1.8	1.51	66
	G	2.00	1.4–2.2	1.79	78
	H	2.30	1.6–2.6	2.04	69
G_p millimhos	C	1.5	3.4–3.6	3.5	2
	E	3.1	3.0–7.0	5.1	76
	F	2.8	2.5–7.0	5.1	66
	G	2.7	2.5–6.5	4.5	70
	H	2.6	2.5–6.5	4.5	69

$G_p \approx (R_{CN}+R_{LN})\omega_0^2 C_N^2 + (R_{Lt}+R_{Cb})/\omega_0^2 L_t^2$ with R_{CN}, R_{Cb} given in Fig. 5, R_{LN}, R_{Lt} given in the Appendix, and $f_0 = \omega_0/2\pi = 3.85$ GHz for E–H circuits and 6.0 GHz for C circuits.

ITDD UTILIZATION IN CIRCULATOR-COUPLED REFLECTION AMPLIFIERS

Basic Design Philosophy

The basic circulator-coupled ITDD reflection amplifier configuration under consideration consists of a tunable narrowband 4 GHz amplifier. It is constructed by connecting a 4 GHz ITDD, mounted as in Fig. 4, through an appropriate length of 50 ohm coaxial line, to the tunable second port of a four-port laboratory model 4 GHz circulator,[3] as shown in Fig. 9(a). A series of these tunable amplifiers, centered at specified frequencies in the 3.7 to 4.05 GHz range, was constructed for use in radio relay systems tests.

The choice for this application of an amplifier having a tunable narrowband rather than a fixed broadband gain-frequency characteristic to cover the 3.7 to 4.05 GHz band was dictated by large signal requirements on an FM radio relay system as well as for reasons of simplicity. Therefore, no attempt was made in this configuration to broadband the amplifier gain by the addition of external matching resonators between the amplifier port of the circulator and the mounted ITDD.

In addition to this amplifier series, a fixed tuned narrowband feasibility model amplifier having the configuration of

[3] Bell Telephone Labs.' F-56880 four-port 4 GHz circulator, which consists of two stripline three-port y-junction circulators in cascade. Two separate tuning screws at the second port of this circulator permit independent adjustment of the input conductance and susceptance at this port. The commercially available 6 GHz circulator is a Western Microwave CYC-993, and the commercially available 4 GHz circulator is a Western Microwave CYC-617.

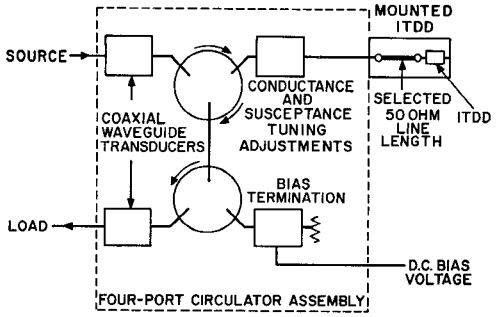

(a) Tunable amplifier.

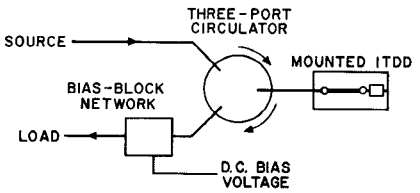

(b) Fixed, tuned feasibility model amplifier.

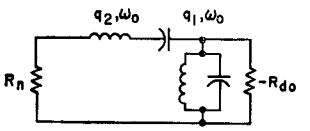

(c) Passband amplifier equivalent circuit at ITDD terminals.

Fig. 9. Experimental ITDD amplifier configurations.

TABLE IV

NOMINAL ITDD DESIGN AND PERFORMANCE PARAMETERS FOR SPECIFIED AMPLIFIER MIDBAND OPERATION

Parameter	Design	
	A	B
Γ_0^2 dB	11	16
R_0 ohms	50	64
f_0 GHz	3.85	6.00
Tunnel diode (Table II)	PB (typ)	PB No. 450
$R_{d0}=R_0[(\Gamma_0+1)/(\Gamma_0-1)]$ ohms	89.5	88
V_b for given R_{d0}mV	115.0	140
$R_{d0(\min)}$ ohms	60	70
β_A required for stability[8]	0.55	0.80
Q_N (Table I) for given $R_{d0(\min)}$ and $R_N=30$ ohms	5.45	3.2
$C_N=Q_N/2\pi f_0 R_{d0}$ pF	2.50	0.96
$L_N=1/4\pi^2 f_0^2 C_N$ nH	0.675	0.735
$C_{d0}(V_b)$ (Table II) pF	0.70	0.40
Fringing and trimming capacity ΔC pF	0.30	0.15
$L_t=1/4\pi^2 f_0^2(C_{d0}+\Delta C)$ nH	1.72	1.28
$C_b>25C_{d0}$ pF	20	20
$Q_0=Q_N+\omega_0 R_{d0}(C_{d0}+\Delta C)$	7.65	5.0
Circulator	F-56880 (typ)	CYC-993
$q_2=q_c$ (meas)	3.00	0
$q_1=q_c'+Q_0 R_0/R_{d0}$	7.00	3.80
Gain shape	SPF	SP
Half power bandwidth $\Delta f=\beta f_0$ MHz	295	440

PB = Pulse bonded simulated beam lead diode [Fig. 7(a)].
SPF = single-peaked tending toward flatness.
SP = Single-peaked.

Fig. 9(b), was constructed at $f_0=6$ GHz. It consisted of an ITDD, centered at f_0, mounted as in Fig. 4, and connected directly to one port of an appropriate three-port commercially available circulator.[3] The purpose of this model was to demonstrate the feasibility of circulator-coupled ITDD amplification at 6 GHz. As before, no attempt was made to broadband the feasibility model amplifier.

Amplifier Design and Performance Calculations

The measured input immittance at the ITDD port of each of the specified circulators[3] is the starting point in the design of the amplifier configurations under consideration. It leads to the determination[8] of the required ITDD active bandwidth, which along with the given tunnel-diode parameters and specified center frequency completely determines the ITDD design. It also influences the resulting passband gain-frequency characteristic both directly by virtue of its passband frequency dependence[8] and indirectly by determining the required value of Q_N and hence, Q_0 (Fig. 1).

Utilizing the measured immittance characteristics of the specified circulators, the required amplifier design calculations are those of the ITDD circuit element values. This assumes that the ITDD uses a specified tunnel diode and is tuned to a specified amplifier center frequency f_0. The following are the required calculations.

1) The tunnel-diode small signal terminal negative resistance level R_{d0}, and the corresponding dc bias voltage V_b (obtained from the I–V characteristic) required for a specified midband gain Γ_0^2 given a fixed circulator midband impedance level R_n such that $R_n<R_{d0}(\min)$ for absolute stability. For cases where R_n is adjustable [Fig. 9(a)], we calculate the value of R_n required for a specified midband gain at R_{d0} corresponding to some optimum V_b (minimum shot noise 20 IR or maximum undistorted output signal level[6]) under the absolute stability constraint $R_n<R_{d0}(\min)$.
2) The thin-film circuit element values which require a prior calculation of the required ITDD active bandwidth and of the corresponding ITDD stabilizing network parameters R_N and Q_N as well as a specification of f_0 and of the tunnel-diode parameters R, R_s, C, and L (Fig. 1).

A complete ITDD design "A" for the tunable 4 GHz amplifier configuration of Fig. 9(a), including specification of nominal values of R_{d0}, V_b, L_t, C_b, R_N, L_N, and C_N is worked out and presented in Table IV for specified midband gain Γ_0^2 at ω_0, for the tunnel-diode parameters in Table II and the measured parameters of the Bell Telephone Labs.' F-56880 circulator. A similar design "B" presented in Table IV for the 6 GHz feasibility model amplifier [Fig. 9(b)], is tailored to use the Western Microwave CYC-993 circulator and available ITDD thin-film circuits.

In each nominal design, no additional matching resonators are interposed between the ITDD and circulator passband immittances, resulting in the passband equivalent circuit at the ITDD terminals shown in Fig. 9(c). Here, reso-

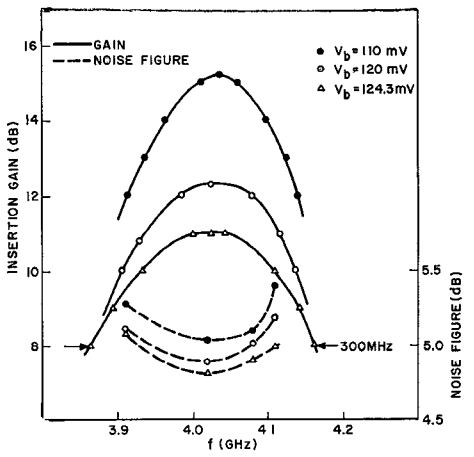

Circulator-BTL F56880 No. 68 Diode-BTL No. 1159
$R_{min}=72.1$ ohms, $C\approx 0.44$ pF, $R_s=2.6$ ohms

Fig. 10. Measured performance of representative 4 GHz tunable ITDD amplifier.

nators q_2 and q_1 include resonators q_c and q_c' (Table IV) which characterize the passband input immittance models[8] of the given circulators.

Calculated bandwidth data for nominal designs A and B, obtained using existing formulations[6],[8] are presented in Table IV along with the relevant ITDD and circulator parameters. It is seen that the calculated gain-frequency characteristic of design B is single peaked, whereas that of design A, while also single peaked, approaches flatness due to the compensating effect of the circulator series resonator q_c. However, it must be emphasized that neither designs A nor B are optimized for a particular gain shape, but are only based on a specified Γ_0^2 and f_0 and on given tunnel-diode and circulator parameters without the interposition of additional matching elements between the circulator and ITDD.

Measured Performance of ITDD Amplifiers

A series of 85 tunable amplifiers having the configuration of Fig. 9(a), tuned to $f_0=3.73$, 3.77, 3.81, 3.85, 3.97, and 4.01 GHz and based on design A were assembled, tuned, and tested prior to their use in systems and environmental tests. Each of these amplifiers was absolutely stable over all values of diode bias voltage and over a wide range of mismatched input and output immittances. Gain and noise figure characteristics of a representative tunable amplifier having ITDD and circulator parameters similar to the nominal values (Table IV) are presented in Fig. 10. Under nominal operating conditions at $f_0=4.01$ GHz, this amplifier exhibits 11.0 dB midband gain, 300 MHz half-power bandwidth, a 60 MHz band about f_0 of flat gain with less than 0.1 dB dropoff, 4.8 dB midband noise figure, and -32 dBm input power level for 1 dB midband gain compression.

The measured performance parameters for the 85 amplifiers under the nominal operating condition of 11 dB midband gain, summarized in Table V, are basically as predicted, with agreement in bandwidth with theory being particularly good. In addition, the measured noise figures

TABLE V
SUMMARY OF MEASURED AMPLIFIER PERFORMANCE

Parameter	Design A	Design B
Circulator	F-56880	CYC-993 No. 10
Tunnel diode	PB	PB No. 450
f_0 GHz	3.73, 3.77, 3.81 3.85, 3.97, 4.01	6.08
Nominal Γ_0^2 dB	11.0	16.1
V_b for nominal Γ_0^2		
range-mV	102–126	140
average-mV	114	
Half-power bandwidth Δf MHz		
range	160–400	440
average	227	
Midband noise figure F dB		
range	4.8–7.1 (4.8–5.8)	5.7
average	6.1 (5.46)	
Δ dB		
range	−1.3 to 1.3 (−0.9 to 0.26)	−0.1
average	−0.44 (−0.42)	
P_{in} dBm		
range	−29 to −38	
average	−34.5	

Δ dB $=F_{meas}$ dB $-F_{calc}$ dB
P_{in} = input power level for 1 dB midband gain compression

Parenthesized values of F and Δ apply to last 20 amplifiers, in which ITDD capacitor electrodes use lower loss gold deposition.

of each of the 85 amplifiers is compared with its theoretical counterpart (Table I), using the individual measured ITDD parameters and the measured circulator insertion losses (0.3 to 0.4 dB). The difference between measured and calculated noise figures, summarized in Table V, indicates good correlation (± 1.3 dB) between these two quantities. The final distribution of measured noise figures (4.8 to 5.8 dB with an average of 5.46 dB) represents a 0.5 to 1.5 dB degradation in amplifier noise figure[4] over that attributable to the diode and circulator alone. The degradation is contributed primarily by the relatively high measured thin-film loss conductances characterizing the devices in question ($G_p\cong 3.3$ to 6.1 millimhos). This noise figure degradation should be reduced as thin-film microwave reactive circuit elements improve in unloaded quality factor and as external components such as circulators develop better controlled out-of-band characteristics. The latter would permit the use of lower stabilizing selectivity in the ITDD and hence would result in lower in-band loss conductance.

In addition, a feasibility model amplifier [Fig. 9(b)] based upon design B and centered at 6 GHz was constructed and tested. This amplifier was absolutely stable over all values of

[4] On the other hand, noise figure degradation introduced by conventional TEM transmission line tunnel-diode amplifier tuning and stabilizing circuitry is typically about 0.5 dB.

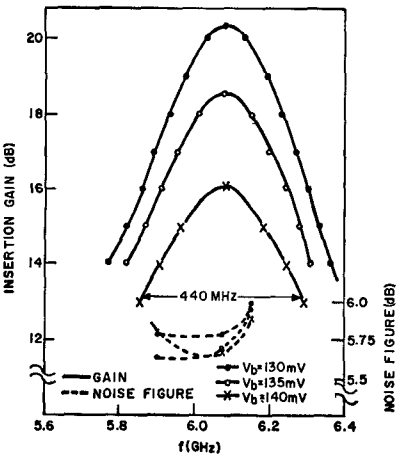

Circulator-Western Microwave CYC-993
Diode-BTL No. 450
$R_{min}=71$ ohms, $C\approx 0.36$ pF, $R_s=2.9$ ohms

Fig. 11. Measured performance of 6 GHz feasibility model ITDD amplifier.

diode bias voltage. Its measured gain and noise figure are presented as functions of frequency for several values of V_b in Fig. 11, and its measured performance parameters are summarized in Table V. Under typical operating conditions for $f_0=6.08$ GHz, this amplifier exhibits 16.1 dB midband gain, 440 MHz half-power bandwidth, and 5.7 dB midband noise figure. The correlation in measured bandwidth and noise figure with theory, as seen in Tables IV and V, respectively, is exceptional. The approximate 1.5 dB degradation in the noise figure of this amplifier over that attributable only to the diode and circulator (0.1 dB insertion loss) is again due to thin-film circuit losses and can be improved upon as stated previously.

Finally, an additional feasibility model amplifier having the configuration of Fig. 9(b) and using a planar[19] tunnel diode on a 4 GHz ITDD and a commercially available 4 GHz three-port circulator[3] was constructed and tested. The resulting amplifier is absolutely stable over the entire active range of tunnel-diode bias voltage. Under typical operating conditions, at $f_0=3.95$ GHz, this amplifier exhibits 10.5 dB midband gain, 6.4 dB midband noise figure, and 170 MHz half-power bandwidth. This amplifier demonstrates the feasibility of using an ITDD containing a planar tunnel diode for reflection amplification.

Conclusions

A series of shunt-tuned integrated microwave tunnel-diode devices utilizing unencapsulated pulse bonded and planar beam lead germanium tunnel diodes and including tuning and stabilizing circuitry, has been fabricated using tantalum thin-film technology. The theoretical properties of such devices have been explored and their design and measured performance described. Finally, the successful use of these devices as the active elements in a series of absolutely stable circulator-coupled reflection amplifiers at 4 and 6 GHz has been demonstrated.

Appendix

Characterization of Coupled Stripline Inductors

The reactance of a short-circuited transmission line of length l, characteristic impedance Z_0, and phase velocity $c/\sqrt{\epsilon}$ (c=velocity of light), given by $X=Z_0 \tan(\omega\sqrt{\epsilon}/c)l$, becomes that of a linear inductor L for $l \ll \pi c/\omega\sqrt{\epsilon}$, such that

$$L \approx \frac{X}{\omega} = \frac{Z_{00}}{c} l; \qquad Z_{00} = Z_0\sqrt{\epsilon} = \lim_{\epsilon \to 1} (Z_0) \tag{1}$$

or

$$L(\text{nH}) \cong 0.0849\, Z_{00}(\text{ohms})\, l\ (\text{inches}).$$

Similarly, the inductance of a cascade of n lines characterized by Z_{0j}, ϵ_j, and l_j ($j=1, 2, \cdots, n$) with the nth line short circuited is given in the short line length limit

$$\left(\sum_{j=1}^{n} l_j\sqrt{\epsilon_j} \ll \frac{\pi c}{2\omega}\right)$$

by

$$L(\text{nH}) \cong 0.0849 \sum_{j=1}^{n} Z_{00j}(\text{ohms})\, l_j\ (\text{inches}) \tag{2}$$

where

$$Z_{00j} = \lim_{\epsilon_j \to 1} (Z_{0j}).$$

The two transmission-line cross sections under consideration here are shown in Fig. 6(a) and (b), and two composite inductor configurations utilizing them are shown in Fig. 6(c) and (d). To determine L for Fig. 6(c) and (d), we must obtain Z_{00} for Fig. 6(a) and (b) and apply the results to (2). Z_{00} is given for the symmetrical coupled-strip configuration of Fig. 6(a) by[17]

$$Z_{00}(\text{ohms}) = 60\pi \frac{K(k')}{K(k)} \tag{3}$$

where

$$K(\alpha) = \int_0^{\pi/2} \frac{d\theta}{\sqrt{1-\alpha^2 \sin^2\theta}}$$

and

$$k = \sqrt{1-k'^2} = \frac{a}{s+a}.$$

The expression for Z_{00} for the cross section of Fig. 6(b)[18] also is that of (3). Therefore, the inductances L_N and L_t of the composite shorted lines of Fig. 6(c) and (d), respectively, obtained by using (3) and (2), are given by

$$L(\text{nH}) \cong 15.95 \sum_{j=1}^{n} \frac{K(k_j')}{K(k_j)} l_j(\text{inches}) \tag{4}$$

where

TABLE VI

PROPERTIES OF COUPLED-STRIPLINE INDUCTORS

Inductor	L_N	L_t			
Design	All	E	F	G	H
l_3 inches	—	0.009	0.016	0.025	0.034
Calculated L nH	1.01	1.78	1.95	2.16	2.38
Measured L nH					
number of samples	4	2	2	2	2
range	0.60–0.74	1.44–1.58	1.76–1.88	1.90–1.96	2.12–2.18
average	0.67	1.51	1.82	1.93	2.15
Calculated R_L ohms	0.28	0.41	0.48	0.58	0.68
Typical measured R_L ohms	—	0.65	0.80	1.0	1.2

$$k_j = \sqrt{1 - k_j'^2} = \frac{a_j}{s_j + a_j} \qquad j = 1, \cdots, n$$

and $n=2$ and 3 for L_N and L_t, respectively.

The series conductor loss resistance associated with each composite inductor may be calculated, noting that the copper-plated conductor thickness ($\approx$0.2 mils) is much greater than the skin depth for copper at 4 GHz ($\approx$0.041 mils), using

$$R_L(\text{ohms}) \approx K_s \sum_{j=1}^{n} \frac{l_{pj}}{a_j} \tag{5}$$

where l_{pj} is the total conductor path length in the jth transmission line ($j=1, 2, \cdots, n$) and, for copper at 4 GHz, surface resistance $K_s \approx 0.0165$ ohms per square.

The calculated and measured properties of five versions of the coupled-stripline inductor configurations used in the ITDD are summarized in Table VI.

ACKNOWLEDGMENT

The success of this effort would not have been possible without the cooperation and assistance of many people at the Bell Telephone Labs. In particular, the author wishes to thank C. N. Dunn, G. Gibbons, and R. E. Davis for supplying the pulse bonded and planar tunnel diodes, respectively, used in these devices, R. Rulison for supplying pulse bonded diodes used in earlier exploratory efforts, and M. D. Bonfeld and his group for supplying the four-port circulators. In addition, the author gratefully acknowledges the assistance of D. A. S. Hale, C. Maggs, E. C. Maslankowski, and B. A. Unger in the fabrication of the integrated devices, related test fixtures, and the amplifiers, of C. French, J. C. Irwin, R. F. Meserve, R. H. Minetti, and H. W. Pacine in doing the required measurements, and of Miss D. M. Bohling and Mrs. M. A. Styczynski in doing related computer calculations. Finally, the author gratefully appreciates the advice and encouragement of W. J. Bertram, who orginally proposed the integrated circuit approach to tunnel-diode amplifier construction.

REFERENCES

[1] H. S. Sommers, Jr., "Tunnel diodes as high-frequency devices," *Proc. IRE*, vol. 47, pp. 1201–1206, July 1959.

[2] T. P. Miles and D. C. Cox, "A microwave tunnel diode amplifier in stripline," *Internat'l Solid-State Circuits Conf., Digest of Tech. Papers*, vol. 8, pp. 24–25, February 1965.

[3] R. C. Havens, "An X-band strip transmission line tunnel diode amplifier," *Microwave J.*, vol. 9, pp. 49–54, May 1966.

[4] J. H. Lepoff and G. J. Wheeler, "Octave bandwidth tunnel-diode amplifier," *IEEE Trans. Microwave Theory and Techniques*, vol. MTT-12, pp. 21–26, January 1964.

[5] R. D. Gallagher, "A microwave tunnel diode amplifier," *Microwave J.*, vol. 8, pp. 62–68, February 1965.

[6] J. Hamasaki, "A low-noise and wide-band Esaki diode amplifier with a comparatively high negative conductance diode at 1.3 Gc/s," *IEEE Trans. Microwave Theory and Techniques*, vol. MTT-13, pp. 213–223, March 1965.

[7] B. T. Henoch and Y. Kvaerna, "Broadband tunnel diode amplifiers," Stanford Electronics Lab., Stanford University, Palo Alto, Calif., Tech. Rept. 213-2, August 1962.

[8] H. C. Okean, "Synthesis of negative resistance reflection amplifiers employing band-limited circulators," *IEEE Trans. Microwave Theory and Techniques*, vol. MTT-14, pp. 323–337, July 1966.

[9] —— "Integrated microwave tunnel diode devices," *Internat'l Microwave Symp. Digest*, pp. 135–140, May 1966.

[10] L. K. Anderson, "Broadband circulators for negative resistance amplifiers," presented at Internat'l Conf. on Microwave Behavior of Ferrimagnetics and Plasmas, London, England, September 13–17, 1965.

[11] B. C. DeLoach, "The noise performance of negative conductance amplifiers," *IRE Trans. Electron Devices*, vol. ED-9, pp. 366–371, July 1962.

[12] T. E. Saunders and P. D. Stark, "An integrated 4 GHz balanced transistor amplifier," *Internat'l Solid-State Circuits Conf., Digest of Tech. Papers*, vol. 9, pp. 18–19, February 1966.

[13] B. A. Unger (private communication).

[14] Meinke and Gundlach, *Taschenbuch der Hochfrequenztechnik*. Berlin, Germany: Springer, 1956, pp. 266–269.

[15] H. C. Okean, "Properties of a TEM transmission line used in microwave integrated circuit applications," *IEEE Trans. Microwave Theory and Techniques* (*Correspondence*), vol. MTT-15, pp. 327–328, May 1967.

[16] V. Ye. Prozorovskiy *et al.*, "Influence of plate resistance on the frequency properties of thin film capacitors," *Telecommun. and Radio Engrg.*, no. 11, pp. 118–123, November 1965.

[17] S. B. Cohn, "Shielded coupled-strip transmission line," *IRE Trans. Microwave Theory and Techniques*, vol. MTT-3, pp. 29–38, October 1955.

[18] R. J. Scudamore (private communication).

[19] G. Gibbons and R. E. Davis, "A beam-lead planar Ge Esaki diode," *Proc. IEEE* (*Letters*), vol. 54, pp. 814–815, May 1966.